Vehicle Height Control of Active Hydro-pneumatic Suspension Considering Ride Comfort

Yizhuang Duan, Zhenle Dong, Dongjie Bai, Zhigang Zhou, Geqiang Li, Shuai Wang

Abstract—**Active hydro-pneumatic suspension has been widely used in heavy vehicles for its extraordinary merits, such as non-linear stiffness and damping, adjustable body height, etc. This paper proposes a vehicle height control method for active hydro-pneumatic suspension considering ride-comfort, a mathematical model of the hydro-pneumatic suspension integrating the dynamics of gas spring (accumulator) and valve-controlled hydraulic system is established, and the control strategy containing model compensation and robust feedback is designed based on backstepping, and the stability of the system is proved via Lyapunov analysis, which shows that the proposed control strategy can theoretically realize the accurate control of vehicle height and limit the acceleration amplitude of the frame. The MATLAB/Simulink platform is used for simulation. The simulation results under the two working conditions show that compared with PID control, the proposed control strategy can achieve higher vehicle height adjustment accuracy and improve vehicle ride comfort.**

Index Terms— **Hydro-pneumatic suspension, vehicle height control, ride comfort, backstepping control**

I. Introduction

Active hydro-pneumatic suspension integrates hydraulic and pneumatic transmission, which has the characteristics of cushioning and vibration reduction, compact structure, and body attitude adjustment [1-3]. Due to the convenience in adjusting the body attitude and improving driving stability and smoothness [4], it has been widely used in engineering practice [5]. With the development of science and technology, people's demands for vehicle driving comfort and the working accuracy of active hydro-pneumatic suspension are gradually increasing. For this, high performance suspension hardware and control strategy are needed as support. Due to the long research and development cycle of suspension hardware, reliable control strategy has become the key to improving the performance of active hydro-pneumatic suspension system.

Active hydro-pneumatic suspension has inherent nonlinear characteristics [6] and parameters perturbation, under different operating conditions, which can bring great difficulties to the design of control strategies. Many scholars have conducted extensive research on this topic. Regarding the non-linearity of stiffness and damping, Ma conducted nonlinear modeling and simulation studies on the hydro-pneumatic suspension system of a certain type of German crane [7]. Zhuang conducted research on the linearization analysis and control strategy for active hydro-pneumatic suspensions [8]. In terms of control strategies, Qin [9] researched the impact of damping diameter and initial inflation volume on vehicle ride smoothness for multi-cylinder hydro-pneumatic suspension systems. Danish [10] proposed an artificial intelligence system capable of real-time monitoring and prediction of hydro-pneumatic suspension performance. Lin [11] introduced fluid inertial mass into the hydro-pneumatic suspension system, achieving ideal damping effects, and designed a model predictive control strategy. Susatio [12] adjusted the PID-controlled active suspension to a second-order system to adapt to changes in the road surface, using a direct synthesis method optimizer to adjust parameters, which allows the control system to adapt to road excitation and achieve desired responses. Chen [13] designed a ride comfort and maneuver stability controller for hydro-pneumatic suspensions based on sliding mode control theory, which can switch between ride comfort controller and maneuver stability controllers under different road surfaces and driving conditions, thus improving ride comfort and maneuver stability controller under several typical steering actions and various road profiles. Kyuhyun [14] used a linear quadratic Gaussian model to propose an optimal control algorithm for semi-active suspension of tractors, and assessed the vehicle's ride comfort based on the comfort index of ISO 2631. Lin [15] proposed a two-stage hierarchical control scheme based

Manuscript received September 2, 2024; revised February 14, 2025.

This work was supported in part by Natural Science Foundation of China under Grant 52305056, in part by Henan Province Science and Technology Research Projects under Grant 242103810050.

Yizhuang Duan is a postgraduate student at the School of Vehicle and Transportation Engineering, Henan University of Science and Technology. Luoyang 471000, China (e-mail: duanyizhuang306@163. com).

Zhenle Dong is an associate professor at the School of Vehicle and Transportation Engineering, Henan University of Science and Technology. Luoyang 471000, China (Corresponding author, e-mail: dong_zhenle@163. com).

Dongjie Bai is a postgraduate student at the School of Vehicle and Transportation Engineering, Henan University of Science and Technology. Luoyang 471000, China (e-mail: b18339631260@163.com).

Zhigang Zhou is a Professor at the School of Vehicle and Transportation Engineering, Henan University of Science and Technology. Luoyang 471000, China (e-mail: hnmczzg@163.com)

Geqiang Li is a professor at the School of Mechatronics Engineering, Henan University of Science and Technology. Luoyang 471000, China (e-mail: hitligeqiang@163.com).

Shuai Wang is a lecturer at the School of Mechatronics Engineering, Henan University of Science and Technology. Luoyang 471000, China (e-mail: wang5451140@163.com).

on MPC control strategy. Qiao [16] proposed a control scheme for timely activation of active hydro-pneumatic suspension and designed a fuzzy PID control system optimized using genetic algorithms. Zhou [17] designed a fault-tolerant control strategy that improves vehicle stability by optimizing the distribution of residual tire forces. Ferhat [18] developed an active suspension system for integrating ride comfort and attitude control of vehicles. Xu [19] studied a system with feedback control and conducted a stability analysis on it. Chen [20] designed an improved based on the active hydro-pneumatic suspension for 6WID UGVs to enhance the vertical stability of UGVs. Zhu [21] develops a new type of semi-active dual-chamber hydro-pneumatic inerter-based suspension. Wei [22] designed a fuzzy control algorithm to reduce errors. Yang [23] linearized the nonlinear characteristics of hydro-pneumatic suspension.

The above studies all start from the vehicle height adjustment. However, in many occasions, it is required that the vehicles have good ride comfort during driving, so it is necessary to take into account ride comfort when designing the vehicle height adjustment controller. Generally, the vehicle height adjustment is mainly realized by the position control of the suspension actuator, and the ride is mainly realized by adjusting the force of the suspension hydraulic actuator, in which conflicts always exist between position control and force control. Therefore, how to take into account the ride comfort when adjusting the vehicle height is a thorny problem in the design of active hydro-pneumatic suspension control strategy.

Based on the above considerations, this paper proposes a vehicle height control method for active hydro-pneumatic suspension considering ride comfort, the mathematical model of the hydro-pneumatic suspension integrating the dynamics of gas spring (accumulator) and valve-controlled hydraulic system is established, and the control strategy containing model compensation and robust feedback is designed based on the backstepping method, and the stability of the system is proved via Lyapunov analysis, which shows that the proposed method can realize the accurate control of the vehicle height and limit the acceleration amplitude of the frame.

II. System Mathematic Models

The structure diagram of the active hydro-pneumatic suspension studied in this paper is shown in Fig. 1.

To facilitate the mathematical modelling of the hydro-pneumatic suspension, the following assumptions are made without affecting its operation: the elastic modulus of hydraulic oil is considered constant, the gas compression process in the accumulator is an adiabatic process; the leaks of gases and liquids throughout the circuit are ignored.

As shown in Fig. 1, one part of the oil in the upper chamber of hydraulic cylinder comes from the accumulator, and the other part comes from the output oil circuit of the servo valve connected with the oil tank, and the two parts can charge or discharge the oil for the hydraulic cylinder at the appropriate time to change its instantaneous pressure, so as to achieve the purpose of height adjustment. The variables in the diagram are defined as follows: m_s denotes 1/4 sprung mass; m_u denotes un-sprung mass; k_t denotes tire vertical elastic stiffness; c_t denotes tire damping; x_r denotes an excitation signal due to the undulation of the road surface; x_u denotes vertical displacement of un-sprung mass; x_s denotes vertical displacement of sprung mass.

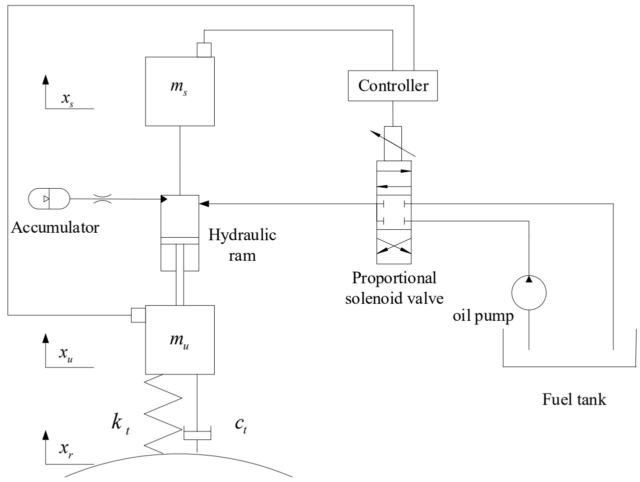

Fig. 1. Structure diagram of 1\/4 active hydro-pneumatic suspension

It is assumed that the cylinder piston is in an equilibrium position at the initial moment $x = 0$, The initial pressure of each hydraulic chamber is: $p_{10} = p_{20}= p_{g0}$, the equation for the balance of forces on the piston rod during operation is

$$m\ddot{x} = p_1 A_1 - mg - f - F_G \tag{1}$$

where m denotes total sprung mass; x denotes piston displacement; A_1, p_1 represent the area of the oil chamber inside the piston and stress state; f denotes the friction between the piston barrel and the piston; F_G indicates the load disturbed by external force.

Defining the direction in which the oil flows into the cylinder is positive, according to the small hole flow equation, the flow rate through the orifice can be calculated as:

$$Q = C_d A \cdot \operatorname{sgn}\left(p_g - p_1\right) \cdot \left(\frac{2 \cdot \left|p_g - p_1\right|}{\rho}\right)^{1/2} \tag{2}$$

where C_d denotes flow coefficient; A denotes the effective flow area of the orifice valve; ρ denotes oil density. The symbolic function is defined as:

$$\operatorname{sgn}\left(x\right) = \begin{cases} 1, x \geq 0 \\ -1, x < 0 \end{cases} \tag{3}$$

The pressure dynamic of the cylinder can be calculated by the following formula:

$$\dot{p}_1 = \frac{\beta_e}{V_{10} + A_1 x}\left(Q - A_1 \dot{x}\right) \tag{4}$$

where β_e denotes the volume of hydraulic oil elastic modulus.

According to ideal gas equation, the state of the gas in the accumulator conforms:

$$p_g v_g^n = p_{g0} v_{g0}^n \tag{5}$$

where n denotes gas adiabatic index, and its value depends on the conditions of the heat exchange process between the gas and the outside world. When the oil and gas spring is working, compared to the gas, the hydraulic oil can hardly be compressed, at this time the gas pressure in the accumulator can be expressed as:

$$p_g = \frac{p_{g0} v_{g0}^n}{\left(v_{g0} + A_1 x\right)^n} \tag{6}$$

According to the above mathematical description of hydro-pneumatic suspension, combined with Newton's second law and the flow-pressure relationship of small holes, the differential equation of the two-degree-of-freedom model of the active hydro-pneumatic suspension can be expressed as:

$$\begin{cases} m_s \ddot{x}_s = A_1 p_1 - c_s\left(\dot{x}_s - \dot{x}_u\right) \\ m_u \ddot{x}_u = -A_1 p_1 - k_t\left(x_u - x_r\right) - c_t\left(\dot{x}_u - \dot{x}_r\right) + c_s\left(\dot{x}_s - \dot{x}_u\right) \\ \dot{p}_1 = \dfrac{\beta_e}{V_{10} + A_1\left(x_s - x_u\right)}\left(Q_g + Q_a - A_1\left(\dot{x}_s - \dot{x}_u\right)\right) \\ Q_g = C_d A_k \cdot \operatorname{sgn}\left(p_g - p_1\right) \cdot \left(\dfrac{2 \cdot \left|p_g - p_1\right|}{\rho}\right)^{1/2} \\ p_g = \dfrac{p_{g0} V_{g0}^n}{\left(V_{g0} + \int Q_g dt\right)^n} \end{cases} \tag{7}$$

where c_s denotes viscous friction coefficient of hydraulic cylinders; Q_g denotes the flow rate through the throttle valve between the cylinder and the air tank; Q_a denotes flow through the valve orifice of the controlled proportional solenoid valve. By charging the proportional solenoid valve, the filling and discharging process of the hydro-pneumatic suspension can be controlled, so as to achieve the purpose of controlling the pressure of hydro-pneumatic suspension.

In order to facilitate the subsequent control design of the active hydrocarbon suspension, the above model needs to be linearized.

The force of the hydraulic cylinder is expressed as

$$\begin{aligned} F_1 = A_1 p_1 &= A_1 p_{g0} + A_1 k_{se} \int Q_a dt - k_{se} A_1^2\left(x_s - x_u\right) \\ &-c_{se} A_1^2\left(\dot{x}_s - \dot{x}_u\right) + A_1 c_{se} Q_a \end{aligned} \tag{8}$$

where constant term $A_1 p_{g0}$ denotes the force exerted on the hydraulic cylinder at the initial moment only by gravity. In the control process, only the dynamic term is generally taken, so the dynamic force of the cylinder piston in the process of movement is obtained as

$$\begin{aligned} F_{1d} &= A_1 k_{se} \int Q_a dt - k_{se} A_1^2\left(x_s - x_u\right) \\ &-c_{se} A_1^2\left(\dot{x}_s - \dot{x}_u\right) + A_1 c_{se} Q_a \end{aligned} \tag{9}$$

The proportional solenoid valve considered in this paper is a fixed-difference pressure-reducing valve installed between the inlet and outlet of a conventional proportional solenoid valve, thus constituting an active control solenoid valve, which can ensure that the input of the solenoid valve is proportional to the flow rate of the valve port and avoid the influence of the pressure difference between the two ends of the solenoid valve. As a result, the flow rate Q_a can be simplified to:

$$Q_a = K_c u \tag{10}$$

where K_c denotes the proportional valve gain.

Based on the above analysis, the dynamic model of the linearized 1/4 vehicle active hydro-pneumatic suspension is as follows:

$$\begin{cases} \ddot{x}_s = \dfrac{A_1 k_{se} \int K_c u dt - k_{se} A_1^2\left(x_s - x_u\right)}{m_s} \\ \quad - \dfrac{c_{se} A_1^2\left(\dot{x}_s - \dot{x}_u\right) + A_1 c_{se} K_c u - c_s\left(\dot{x}_s - \dot{x}_u\right)}{m_s} \\ \ddot{x}_u = \dfrac{k_{se} A_1^2\left(x_s - x_u\right) - A_1 k_{se} \int K_c u dt - A_1 c_{se} K_c u}{m_u} \\ \quad + \dfrac{c_{se} A_1^2\left(\dot{x}_s - \dot{x}_u\right) - k_t\left(x_u - x_r\right)}{m_u} \\ \quad + \dfrac{c_s\left(\dot{x}_s - \dot{x}_u\right) - c_t\left(\dot{x}_u - \dot{x}_r\right)}{m_u} \\ p_1 = p_{g0} + k_{se} \int K_c u dt - k_{se} A_1\left(x_s - x_u\right) \\ \quad -c_{se} A_1\left(\dot{x}_s - \dot{x}_u\right) + c_{se} K_c u \end{cases} \tag{11}$$

III. Controller Design

Let $x_1 = x_s$, $x_2 = \dot{x}_s$, $x_3 = x_u$, $x_4 = \dot{x}_u$, $x_5 = \dot{x}_2$, then the above kinetic model can be represented as:

$$\begin{cases} \dot{x}_1 = x_2 \\ \dot{x}_2 = x_6 \\ \dot{x}_6 = \dfrac{A_1 k_{se} K_c u}{m_s} - \dfrac{A_1^2 k_{se}\left(x_2 - x_4\right)}{m_s} \\ \quad - \dfrac{A_1^2 c_{se}\left(\dot{x}_2 - \dot{x}_4\right)}{m_s} + \dfrac{A_1 c_{se} K_c \dot{u}}{m_s} - \dfrac{c_s\left(\dot{x}_2 - \dot{x}_4\right)}{m_s} \\ \dot{x}_3 = x_4 \\ \dot{x}_4 = \dfrac{k_{se} A_1^2\left(x_1 - x_3\right) - A_1 k_{se} \int K_c u dt - A_1 c_{se} K_c u}{m_u} \\ \quad + \dfrac{c_{se} A_1^2\left(x_2 - x_4\right) - k_t\left(x_3 - x_r\right)}{m_u} \\ \quad + \dfrac{c_s\left(x_2 - x_4\right) - c_t\left(x_4 - \dot{x}_r\right)}{m_u} \end{cases} \tag{12}$$

The purpose of controller design is to control the height of the suspension as accurately as possible, while limiting the frame acceleration, that is, designing a controller u, making body height status x_1 approach to x_{1r}, and ensuring that vehicle body vertical acceleration state x_6 is limited to a certain value, wherein x_{1r} is the height virtual control input.

Controller design is divided into the following 4 steps.

Step 1: Let $e_1 = x_1 - x_{1r}$, $e_2 = x_2 - x_{2r}$, where x_{2r} is the virtual control input for velocity, then the vehicle height error dynamics can be expressed as:

$$\dot{e}_1 = \dot{x}_1 - \dot{x}_{1r} = x_2 - x_{1r} = e_2 + x_{2r} - \dot{x}_{1r} \tag{13}$$

Defining $x_{2r} = -k_1 e_1 + \dot{x}_{1r}$, where k_1 is a positive controller parameter, then we have

$$\dot{e}_1 = -k_1 e_1 + e_2 \tag{14}$$

By defining the Lyapunov function $V_1 = \frac{1}{2} e_1^2$, we have:

$$\dot{V}_1 = e_1 \dot{e}_1 = -k_1 e_1^2 + e_1 e_2 \tag{15}$$

When $|e_2| \le E_2$ (E_2 will be designed in the subsequent process), we have:

$$\dot{V}_1 \le -k_1 e_1^2 + \frac{E_2^2 e_1^2}{4\eta_1} + \eta_1 = -\left(k_1 - \frac{E_2^2}{4\eta_1}\right) e_1^2 + \eta_1 \quad (16)$$

where η_1 is an arbitrarily small positive constant, and when $k_1 > \frac{E_2^2}{4\eta_1}$, we have

$$\dot{V}_1 \le -k_1 e_1^2 + \frac{E_2^2 e_1^2}{4\eta_1} + \eta_1 = -\left(k_1 - \frac{E_2^2}{4\eta_1}\right) e_1^2 + \eta_1 \quad (17)$$

where $\tilde{k}_1 = k_1 - \frac{E_2^2}{4\eta_1}$, and then the integration of $\dot{V}_1$ yields:

$$V_1(t) \le \frac{\eta_1}{2\tilde{k}_1} + \left(V_1(0) - \frac{\eta_1}{2\tilde{k}_1}\right) e^{-2\tilde{k}_1 t} \quad (18)$$

and when $t \to \infty$, we have $\left| e_1(\infty) \le \sqrt{\frac{\eta_1}{\tilde{k}_1}} \right|$

Step 2: Let $e_6 = x_6 - x_{6r}$, where x_{6r} is the virtual control input for acceleration, then the vehicle speed of dynamics of error e_2 can be expressed as:

$$\dot{e}_2 = \dot{x}_2 - \dot{x}_{2r} = x_6 - \dot{x}_{2r} = e_6 + x_{6r} - \dot{x}_{2r} \quad (19)$$

Defining $x_{6r} = -k_2 e_2 + \dot{x}_{2r}$,where k_2 is a positive controller parameter, then we have

$$\dot{e}_2 = -k_2 e_2 + e_6 \quad (20)$$

By defining the Lyapunov function $V_2 = \frac{1}{2} e_2^2$, we have:

$$\dot{V}_2 = e_2 \dot{e}_2 = -k_2 e_2^2 + e_2 e_6 \quad (21)$$

When $|e_6| \le E_6$ (E_6 will be designed in the subsequent process), we have:

$$\dot{V}_2 \le -k_2 e_2^2 + \frac{E_6^2 e_2^2}{4\eta_2} + \eta_2 = -\left(k_2 - \frac{E_6^2}{4\eta_2}\right) e_2^2 + \eta_2 \quad (22)$$

where η_2 is an arbitrarily small positive constant, and when $k_2 > \frac{E_6^2}{4\eta_2}$, we have

$$\dot{V}_2 \le -\tilde{k}_2 e_2^2 + \eta_2 = -2\tilde{k}_2 V_2 + \eta_2 \quad (23)$$

where $\tilde{k}_2 = k_2 - \frac{E_6^2}{4\eta_2}$, and then the integration of $\dot{V}_2$ yields:

$$V_2(t) \le \frac{\eta_2}{2\tilde{k}_2} + \left(V_2(0) - \frac{\eta_2}{2\tilde{k}_2}\right) e^{-2\tilde{k}_2 t} \quad (24)$$

so when $t \to \infty$, we have: $\left| e_2(\infty) \le \sqrt{\frac{\eta_2}{\tilde{k}_2}} \right|$

Step 3: The dynamics of e_6 are expressed as:

$$\begin{aligned}\dot{e}_6 = \dot{x}_6 - \dot{x}_{6r} &= \frac{A_1 k_{se} K_c u}{m_s} - \frac{A_1^2 k_{se}(x_2 - x_4)}{m_s} \\ &- \frac{A_1^2 c_{se}(\dot{x}_2 - \dot{x}_4)}{m_s} + \frac{A_1 c_{se} K_c \dot{u}}{m_s} - \frac{c_s(\dot{x}_2 - \dot{x}_4)}{m_s} - \dot{x}_{6r}\end{aligned} \quad (25)$$

Define

$$\begin{aligned}u &= \frac{A_1(x_2 - x_4)}{k_c} + \frac{c_{se} A_1(\dot{x}_2 - \dot{x}_4)}{k_{se} k_c} - \frac{c_{se}\dot{u}}{k_{se}} \\ &+ \frac{m_s}{A_1 k_{se} k_c}\dot{x}_{6r} - \frac{k_6 m_s}{A_1 k_{se} k_c} e_6 + \frac{c_s(x_6 - \dot{x}_4)}{A_1 k_{se} k_c},\end{aligned}$$

where k_6 is a positive controller parameter, then we have

$$\dot{e}_6 = -k_6 e_6 \quad (26)$$

By defining the Lyapunov function $V_6 = \frac{1}{2} e_6^2$, we have:

$$\dot{V}_6 = e_6 \dot{e}_6 = -k_6 e_6^2 \quad (27)$$

so the system is stable, and the existence of E_6 makes $|e_6| \le E_6$

According to $\dot{V}_2 \le -2\tilde{k}_2 V_2 + \eta_2$ and $|e_6| \le E_6$, we can get

$$|e_2(t)| \le \max\left\{\sqrt{\frac{\eta_2}{\tilde{k}_2}}, e_2(0)\right\} = E_2 \quad (28)$$

Further, according to $\dot{V}_1 \le -2\tilde{k}_1 V_1 + \eta_1$ and $|e_2| \le E_2$, we can get

$$|e_1(t)| \le \max\left\{\sqrt{\frac{\eta_1}{\tilde{k}_1}}, e_1(0)\right\} = E_1 \quad (29)$$

Combine equation and

$$\dot{x}_{2r} = -k_1 \dot{e}_1 + \ddot{x}_{1r}, \dot{e}_1 = -k_1 e_1 + e_2 \quad (30)$$

In summary, x_6 can be expressed as:

$$x_6 = e_6 + x_{6r} = e_6 - (k_1 + k_2) e_2 + k_1^2 e_1 + \ddot{x}_{1r} \quad (31)$$

From the above equation, it can be seen that if $|\ddot{x}_{1r}| \le X_{1rm}$ then there is:

$$|x_6| \le E_6 + (k_1 + k_2) E_2 + k_1^2 E_1 + X_{1rm} \le X_6 \quad (32)$$

where E_1, E_2, E_6 denotes the upper limit of the error that needs to be guaranteed in the design process; X_{1rm} is the upper bound of the height virtual control input.

Step 4: When $\ddot{e}_1 = \dot{e}_2 = e_6 = 0$, zero dynamics of the considered system can be expressed as:

$$\begin{cases}\dot{x}_3 = x_4 \\ \dot{x}_4 = \dfrac{-m_s \ddot{x}_{1r} - k_t(x_3 - x_r) - c_t(x_4 - \dot{x}_r) + c_s(\dot{x}_{1r} - x_4)}{m_u}\end{cases} \quad (33)$$

The above equation can be turned into:

$$\begin{aligned}&\ddot{x}_3 + \frac{c_t}{m_u}\dot{x}_3 + \frac{k_t}{m_u}x_3 + \frac{m_s \ddot{x}_{1r}}{m_u} - \\ &\frac{k_t}{m_u}x_r - \frac{c_t}{m_u}\dot{x}_r + \frac{c_s}{m_u}\dot{x}_{1r} + \frac{c_s}{m_u}\dot{x}_3 = 0\end{aligned} \quad (34)$$

and characteristic equation is:

$$s^2 + \left(\frac{c_t + c_s}{m_u}\right) s + \frac{k_t}{m_u} = 0 \quad (35)$$

where $c_t > 0$, $c_s > 0$, $m_u > 0$, $k_t > 0$, So we have $\frac{c_t + c_s}{m_u} > 0, \frac{k_t}{m_u} > 0$,and the coefficients of the characteristic equations of the second-order zero-dynamic system are all positive, so the zero-dynamic system (33) is stable, i.e., when the road vertical input x_r, $\dot{x}_r$, and the reference signal $\ddot{x}_{1r}$ are bounded, x_3, x_4 are bounded.

IV. Simulation and Analysis

MATLAB/Simulink is used to verify the effectiveness of the proposed vehicle height control method for active hydro-pneumatic suspension considering ride comfort. The control strategy proposed in this paper is implemented through the s-function module, which is written in C++ language and can run directly. The suspension parameters of 1/4 of the vehicle used in this simulation are shown in Table 1.

TABLE I
PARAMETERS OF MOTOR SERVO SYSTEM

Symbol	Value	Symbol	Value
m_s	2137*kg*	k_t	704000*N/m*
m_u	3750*kg*	c_t	3362*Ns/m*

To verify the advantages of the proposed strategy in the longitudinal comfort of the vehicle height process, PID control strategy, which is widely used in engineering, is selected for comparison.

Two road conditions are selected for simulation analysis, i.e., sinusoidal excitation pavement and random excitation pavement.

A. Sinusoidal excitation road surface

The vehicle height is adjusted in the environment where the road face excitation is $z_r(t) = 0.01\sin(2\pi t)$, which is added from 2s to the 6s, and the vehicle height rises from 0 to 0.02m. During the simulation, all states are initialized to 0, and the sampling time is 0.0005s. In this case, the controller parameters are selected as: $k_1 = 30$, $k_2 = 20$, $k_6 = 30$, and set the PID parameters are set as $k_p = 100$, $k_i = 120$, $k_d = 110$.

The simulation results are shown in Fig. 2-5, where "controller 1" is the proposed controller, and "controller 2" is PID controller.

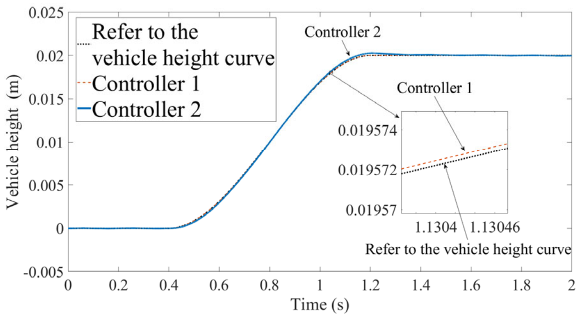

Fig. 2. Curves of the vehicle body height

Fig. 2 is the vehicle height tracking curve of the two controllers, and Fig. 3 is the error curve of the two controllers. As can be seen from Fig. 2 the proposed vehicle height control method can track the reference vehicle height curve with a smaller error than PID algorithm. As can be seen from Fig. 3 the maximum tracking error of proposed vehicle height control method is about 1.4×10^{-3} m to 4×10^{-4} m, reduced by 71% compared with PID controller.

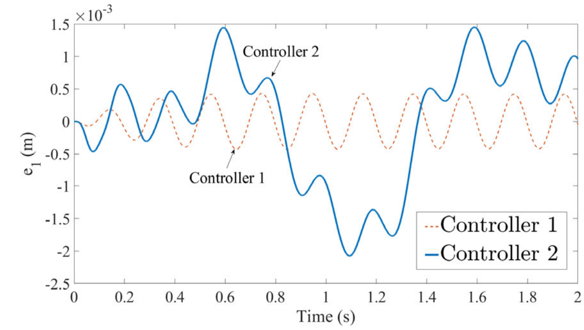

Fig. 3. Curves of tracking error of the vehicle body height

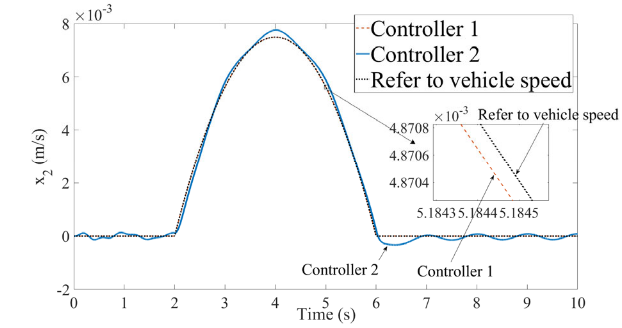

Fig. 4. Curves of the vehicle body velocity

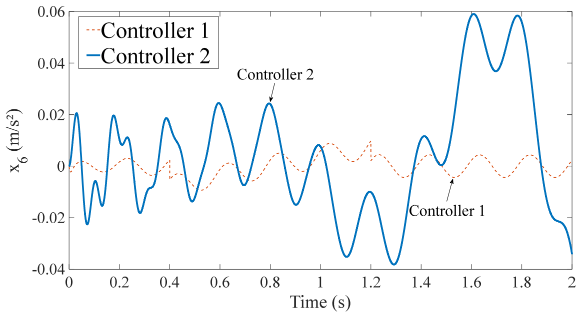

Fig. 5. Curves of the vehicle body acceleration

TABLE II
PERFORMANCE INDICES FOR HEIGHT REGULATION (SINUSOIDAL EXCITATION ROAD SURFACE)

Index	Controller 1	Controller 2
e_1/m	4×10^{-4}	1.4×10^{-3}
x_6/(m/s^2)	4.3×10^{-3}	3.7×10^{-2}

Fig. 4 shows the speed curve of vehicle body of the two controllers. It can be seen from Fig. 4 that the proposed control strategy can track the reference body speed curve accurately, and a large error will be generated when PID controller is used, especially the relatively violent jitter in the beginning and end stages, which may cause poor ride in the process of vehicle height adjustment. Fig. 5 shows the body acceleration curves under two different control algorithms. It can be seen that the body acceleration amplitude of the proposed control is 0.0087 m/s^2, which is within the acceleration limit; whereas the body acceleration amplitude of PID controller reaches to 0.058 m/s^2, exceeding the acceleration limit. So, the proposed control strategy achieves a performance improvement of 98.5% over the PID control strategy.

B. Random excitation road surface

In this case, the influence of a random road excitation, is considered. The Fig. 6 shows the image of the random road signal. From 2s to 6s. During this period, the vehicle height is reduced from 0.02 to 0, all states are initialized to 0, and the sampling time is set at 0.0005s. Under these conditions, the controller parameters are selected as: $k_1 = 20$, $k_2 = 100$, $k_6 = 100$, and set the PID controller parameters are set as: $k_p = 100$, $k_i = 400$, $k_d = 600$.

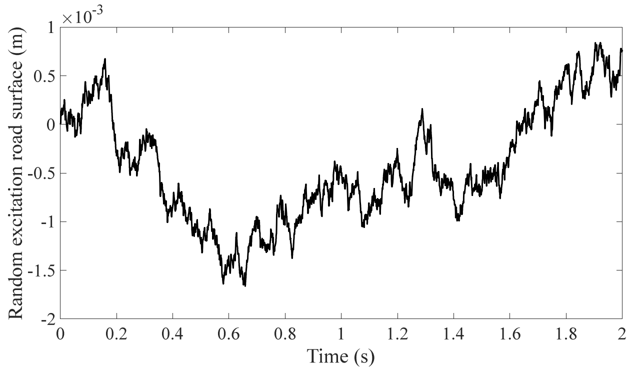

Fig. 6. The random road signal

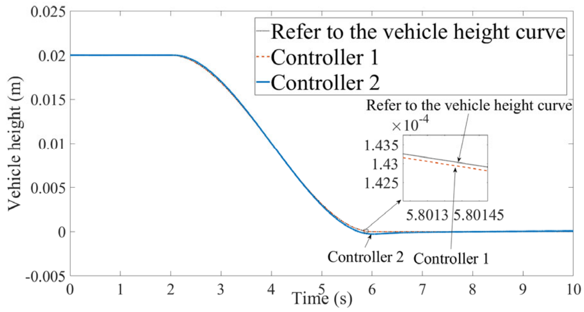

Fig. 7. Curves of the vehicle body height

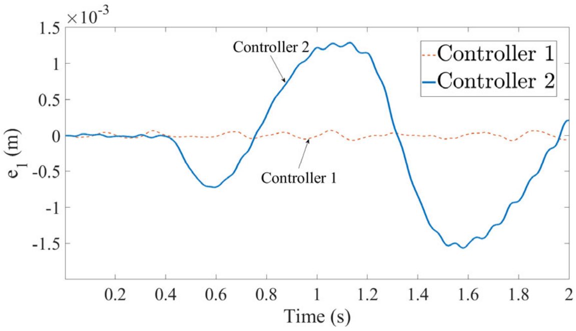

Fig. 8. Curves of tracking error of the vehicle body height

The vehicle height tracking curve of the two controllers is shown in Fig. 7, and the curve of tracking errors of the two controllers is shown in Fig. 8. As can be seen from Fig. 7, the reference vehicle height curve can be tracked with a smaller error by the proposed vehicle height control strategy compared to the PID algorithm. As shown in Fig. 8, the maximum tracking error of the proposed vehicle height control method is reduced from 1.2×10^{-3} m to 7.2×10^{-5} m, representing a 94% reduction compared to the PID controller. Fig. 9 shows the speed curve of vehicle body of the two controllers. It can be seen that the proposed control strategy can better track the reference body speed curve, especially the relatively violent jitter in the beginning and end stages, which may cause poor ride in the process of vehicle height adjustment.

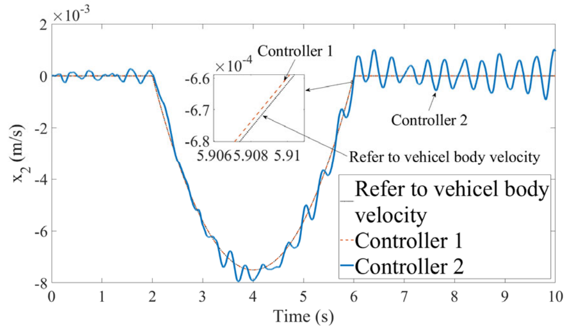

Fig. 9. Curves of the vehicle body velocity

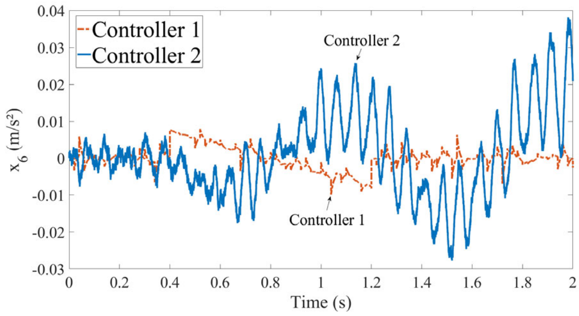

Fig. 10. Curves of the vehicle body acceleration

TABLE III

PERFORMANCE INDICES FOR HEIGHT REGULATION (RANDOM EXCITATION ROAD SURFACE)

Index	Controller 1	Controller 2
e_1/m	7.2×10^{-5}	1.2×10^{-3}
x_6/(m/s²)	4.3×10^{-3}	3.7×10^{-2}

The body acceleration curves under two different control strategy are shown in Fig. 10. It can be seen that the body acceleration amplitude of the proposed control is 0.0043 m/s², which is within the acceleration limit, whereas the body acceleration amplitude of the PID controller reaches 0.037m/s², exceeding the set limit. Therefore, a performance improvement of 88.3% over the PID control strategy can be achieved by the proposed control strategy.

V. CONCLUSION

This paper proposed a vehicle height control method for active hydro-pneumatic suspension considering ride-comfort and the stability of the controller is proved via Lyapunov analysis. The results show that under two road conditions, regardless of the vehicle height is raised or lowered, the proposed controller can better track the reference vehicle height curve compared with PID controller. Moreover, the acceleration can also be controlled within the allowable limit. So, the proposed control strategy can improve safety and stability to complex road conditions. The focus of future research will be placed on further considering system parameter deviations, and an attempt will be made to apply the proposed controller to the actual operation of vehicles.

REFERENCES

[1] L. WANG, B. ZHAO, D. LI, and L. LIU, "Simulation of Hydro-pneumatic Suspension and Vehicle Dynamics System of Wide Body Truck for Mine," *Chinese Hydraulics & Pneumatics*, vol. 48, no. 11, pp. 158-163, 2020.

[2] Y. Song, L. Liu, Z. Li, J. Lian, J. Meng, and B. Yan, "Research on modeling and behavioral characteristics of bionic kangaroo leg suspension with circular Arc-Buffer structures," *Journal of Xi'an Jiaotong University*, vol. 55, no. 9, pp. 28-38, 2021.

[3] X. LIU, and Y. LI," Review of Research Methods of Vehicle Hydro-Pneumatic Suspension Technology, "*Journal of Southwest Jiaotong University*, vol. 71, no. 6, pp. 1-20, 2023.

[4] Lv, K., J. Wang, H. Cheng, H. Wang, and J. Wang," Modeling of hydro-pneumatic suspension system with fractional order terms and simulation analysis of road friendliness," *Proceedings of the Institution of Mechanical Engineers Part D-Journal of Automobile Engineering*, vol. 237, no. 10-11, pp. 2605-2615, 2023.

[5] L. Yang, "Research on Longitudinal-Lateral-Vertical Coordinated Control of Active Hydro-pneumatic Suspension for Engineering Vehicles," Ph.D. dissertation, Dept. Automobile. Eng., Jiangsu Univ., Jiangsu, China, 2021.

[6] S. Li, "Nonlinear modeling and adaptive control of active hydro-pneumatic suspension," M.S. thesis, Dept. Automobile. Eng., Yanshan Univ., Hebei, China, 2019.

[7] Q. Ma, H. Tan, and M. Wu " Study on the Quarter Vehicle Mathematical Model Based on Hydro-pneumatic Suspension," *Journal of Hebei University of Technology*, vol. 31, no. 6, pp. 30-34, 2002.

[8] J. Zhuang, "Study on vertical and lateral dynamic performances of vehicle with active hydro-pneumatic suspension," Ph.D. dissertation, Dept. Automobile. Eng., Shanghai Jiao Tong Univ., Shanghai, China, 2021.

[9] Qin, B., R. Zeng, X. Li, and J. Yang, "Design and Performance Analysis of the Hydro-pneumatic Suspension System for a Novel Road-Rail Vehicle, " *Applied Sciences-Basel*, vol. 11, no. 5, pp. 2221, 2021.

[10] Ali, D., and S. Frimpong," Artificial intelligence models for predicting the performance of hydro-pneumatic suspension struts in large capacity dump trucks," *International Journal of Industrial Ergonomics*, vol. 67, pp. 283-295, 2018.

[11] Yang, L., R.C. Wang, R.K. Ding, W. Liu, and Z.H. Zhu," Investigation on the dynamic performance of a new semi-active hydro-pneumatic inerter-based suspension system with MPC control strategy, "*Mechanical Systems and Signal Processing*, vol. 154, pp. 107569, 2021.

[12] Susatio, Y., L. Oktaviana, N.K. Rizki, E. Listijorini, and T.R. Biyanto, "Design of half-car active suspension system for passenger riding comfort," *Journal of Physics: Conference Series*, vol. 1075, no. 1, pp. 012030, 2018.

[13] Zhou, C., X. Liu, F. Xu, and W. Chen," Sliding Mode Switch Control of Adjustable Hydro-Pneumatic Suspension based on Parallel Adaptive Clonal Selection Algorithm," *Applied Sciences-Basel*, vol. 10, no. 5, pp. 1852, 2020.

[14] Sim, K., H. Lee, J.W. Yoon, C. Choi, and S.-H. Hwang," Effectiveness evaluation of hydro-pneumatic and semi-active cab suspension for the improvement of ride comfort of agricultural tractors," *Journal of Terramechanics*, vol. 69, pp. 23-32, 2017.

[15] Yang, L., J.W. Zhang, and S.Z. Chen, "Research on Hydro-Pneumatic Balanced Suspension of Multi-Spindled Vehicle", *International Conference on Mechanical Materials and Manufacturing Engineering*, vol. 66-68, pp. 855-861, 2011.

[16] Qiao, C., H. Wen, X. Liu, and G. Wang," Damping Control and Experiment on Active Hydro-Pneumatic Suspension of Sprayer Based on Genetic Algorithm Optimization," *Frontiers in Neurorobotics*, vol. 15, 2021.

[17] Zhigang Zhou, Xinqing Ding, Zhichong Shi, Xiaofei Yin, and Xiangming Meng, "In-wheel Motor Electric Vehicle Based on Fuzzy Neural Network Yaw Stability Optimization Control," Engineering Letters, vol. 31, no.4, pp1717-1723, 2023.

[18] Saglam, F., and Y.S. Unlusoy, " Adaptive ride comfort and attitude control of vehicles equipped with active hydro-pneumatic suspension," *International Journal of Vehicle Design*, vol. 71, no. 1-4, pp. 31-51, 2016.

[19] Lili Xu, Yalong Xue, Qifa Lin, and Fengde Chen, "Stability and Bifurcation Analysis of Commensal Symbiosis System with the Allee Effect and Single Feedback Control," IAENG International Journal of Applied Mathematics, vol. 54, no. 8, pp1586-1596, 2024.

[20] Chen, G., Y. Jiang, Y. Tang, and X. Xu," Revised adaptive active disturbance rejection sliding mode control strategy for vertical stability of active hydro-pneumatic suspension," *ISA Transactions*, vol. 132, pp. 490-507, 2023.

[21] Zhu, Z., R. Wang, L. Yang, Z. Sun, and X. Meng," Modelling and control of a semi-active dual-chamber hydro-pneumatic inerter-based suspension system," *Proceedings of the Institution of Mechanical Engineers, Part D: Journal of Automobile Engineering*, vol. 235, no. 9, pp. 2355-2370, 2021.

[22] Yuan Wei, Haoran Li, Zhigang Zhou, and Dongdong Chen, "Driving Path Tracking Strategy of Humanoid Robot Based on Improved Pure Tracking Algorithm," IAENG International Journal of Applied Mathematics, vol. 54, no. 2, pp286-297, 2024.

[23] Yang, F., Y. Du, X. Li, Y.a. Zhang, E. Mao, and Z. Li, "Active Suspension Control and Experimental Research of Large Sprayer with Multi-operating Conditions Integrating Road Characteristics," *Nongye Jixie Xuebao/Transactions of the Chinese Society for Agricultural Machinery*, vol. 54, pp. 110-120, 2023.